ANALYSIS OF UAVs FLIGHT CHARACTERISTICS

Vasile PRISACARIU

"Henri Coandă" Air Force Academy, Braşov, Romania (aerosavelli73@yahoo.com)

DOI: 10.19062/1842-9238.2018.16.3.4

Abstract: *The analysis of flight characteristics of aircraft using freeware tools is used both for educational and research purposes, but especially for computing, construction and manufacturing in the commercial and hobby area. XFLR provides aerodynamic analysis capabilities for non-propulsion aircraft with reasonable results.*

The article presents 2D and 3D analyzes of the UAV geometry in a classic concept, with a presentation of the numerical differences in flight characteristics for four cases on the profiles used in the wing.

Keywords: *aerodynamic analysis, UAV, XFLR5, flight parameter.*

Acronyms and symbols

CFD	*Computational Fluid Dynamics*	*AR*	*Aspect Ratio*
LLT	*Lifting Line Theory*	*VLM*	*Vortex Lattice Method*
XFLR	*Xfoil Low Reynolds*	ρ	*Air density*
c_l, c_d,c_m,c_y	*Aerodynamic coefficient*	C_L/C_D	*Gliding ratio*
AoA, alpha	*Angle of incidence*		

1. INTRODUCTION

Since 2007, XFLR5 has become an open source development project hosted by Sourceforce.net and has been designed exclusively for designing non-propulsion aerodynamic models (without the influence of rotating lifting surfaces/propellers) for which it provides reasonable and consistent results [1].

According to the specialty references [2, 4, 5, 6, 7, 8], the use of XFLR5 is now widely spread both in the educational, research and hobby area. It can perform analyzes for small Reynolds numbers using a series of geometry/comparison Design applications, aerodynamic analysis (2D and 3D) and stability analysis.

The 2D and 3D analysis steps based on three known methods: LLT, VLM and 3D panels are as follows: geometric 2D configuration (aerodynamic profile) by generating NACA profiles or importing a profile from external databases; 2D profile analysis; geometric 3D configuration (fuselage, empennage; wings); 3D analysis on single elements; 3D analysis on complete geometry (considering interferences); stability analysis (with inertial mass values). The results can be viewed graphically or numerically (data export) using three options for the polarities of the analyzed geometry: constant speed, constant lift, constant incidence, [1].

The following is an aerodynamic analysis of a unique geometric configuration (non-propulsion aircraft/glider) based on four aerodynamic profiles for the main lifting surface (wing), an analysis that wishes to highlight the performance differences of the four analyzed profiles.

2. GEOMETRIC CONFIGURATION

The geometric definition of a fixed-wing UAV assumes the same systematic approach as in the case of a aircraft with pilot, that is to say the first aerodynamic concept chosen is implemented according to the main assignment attributed to the air vector, then refined geometric optimization on each main component element (fuselage, wing, empennage).

XFLR5 [1, 4] provides geometric parameterization tools for both rotation (fuselage) and lifting surfaces (wing, empennage). The user interface is intuitive and provides both numeric editing areas (FIG. 1a) and graphics and final geometry information (FIG. 1b).

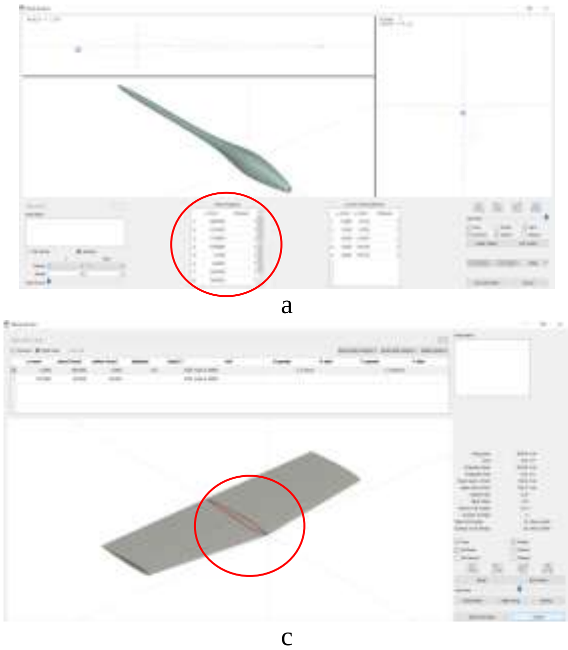

FIG. 1. Geometric configuration of UAV, a.fuselage, b. wing, c.horizontal tail, d. vertical tail

The numerical setting of geometric parameters provides in real time 2D and 3D graphical changes (3 views and isometric view) of the parameterized object (FIG. 1c). For additional information, you can use the upper-right editing field of the geometric submenus (FIG. 1d).

3. 2D AERODYNAMCS ANALYSIS

2D aerodynamic analyzes were performed on four known aerodynamic profiles, mainly used in tailless (fly wing) aircraft as shown in FIG. 2 and the conditions in Table 1, profiles having different geometric characteristics on the skeleton, thickness and arrow (curvature). [3]

Table 1.Analysis conditions

Parameter	Value	Parameter	Value
AoA range	-5..15^o	Nr. Reynolds Re	684000
Air density ρ	1,225 kg/m^3	Cinematic viscosity	1,46x10^{-5} m^2/s
Iterations	100	Viscosity / boundary layer	activ / activ
Chord	1 m	Analysis type	constant speed

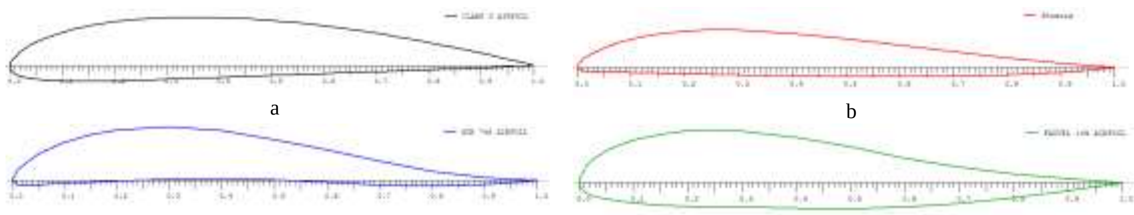

a b c d

FIG. 2 Airfoils, a.Clark Y, b.Phoenix, c.GOE 746, d.Fauvel 14%

Airfoils analyzed over the incidence range -5° ÷ 15° produced comparative polar highlighted in the figures below, the numerical data taken into account the viscous effects of the flow.

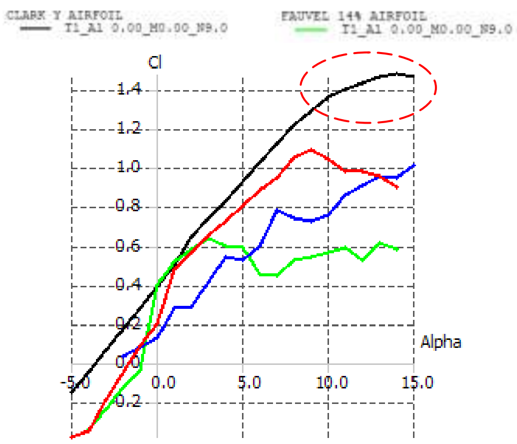

FIG. 3. C_l vs AoA

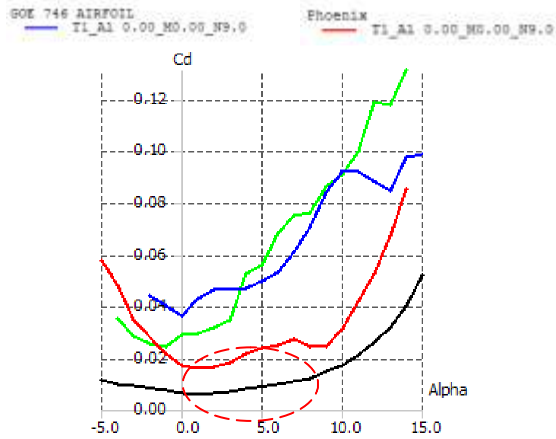

FIG. 4. C_d vs AoA

The lift coefficient polar (C_l-AoA) provides higher values for the Clark Y profile over the entire incidence range -5° ÷ 15° with a maximum of 1.47 at AoA = 14° (see Figure 3 and Table 2). The drag is also minimal for Clark Y having a value of 0.006 to AoA = 1°, see FIG. 3.

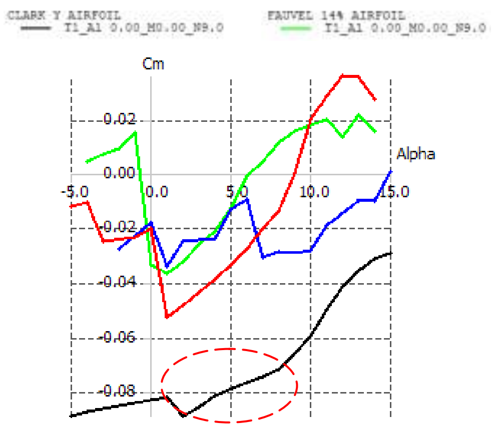

FIG 5. C_m vs AoA

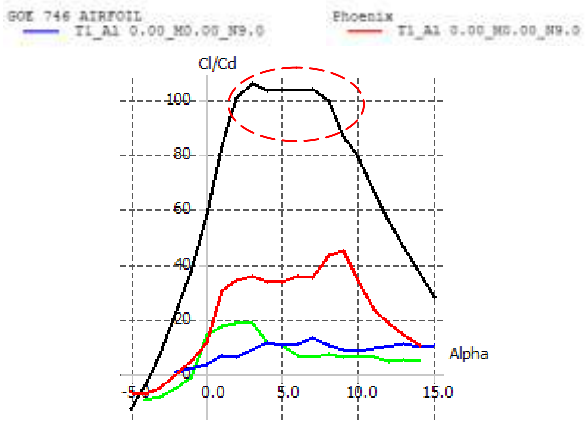

FIG. 6 Finețea C_l/C_d vs AoA

The pitch coefficient C_m (FIG. 5 and Table 2) on a positive incidence offered by Clark Y is 0.085 to AoA = 3° although a local error of calculation can be speculated in view of this isolated maximum value, and for GOE 746 and Fauvel 14% shows values indicating auto-stable behavior. The theoretical aerodynamic fineness (glider ratio) has maximum values for Clark Y over 100 units per AoA = 3° ÷ 7° and for the other airfoils under 50 units, FIG. 6.

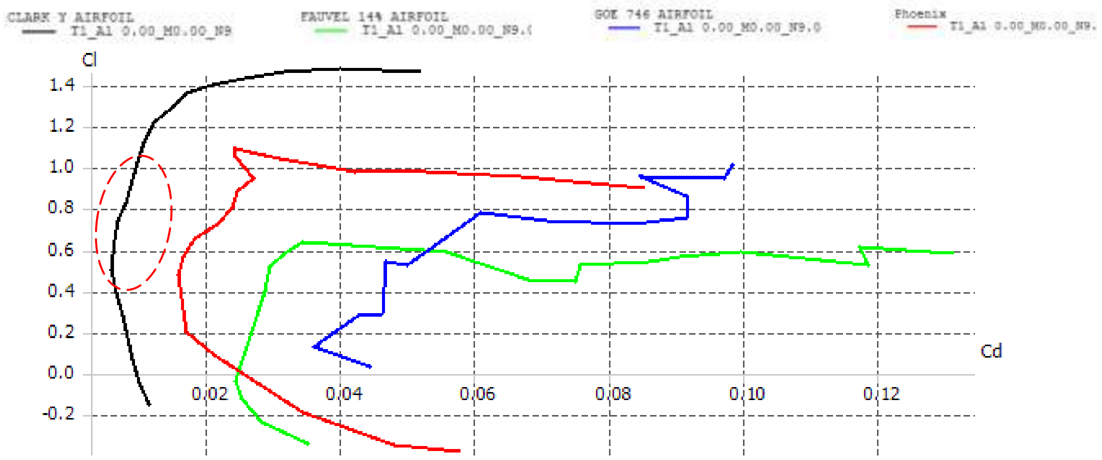

FIG. 7 C_l vs C_d

The polar C_l-C_d (FIG. 7) indicates optimal aerodynamic behavior for Clark Y in terms of minimum drag (C_d = 0,01) coupled with values of the lift coefficient (C_l = 0,49) corresponding to AoA = 1^0, while for AoA = 14^o (critical incidence) we have C_d = 0.039.

Table 2.Airfoils numeric values

Clark Y	*Fauvel 14%*
[illegible]	[illegible]

In the aerodynamic 2D conception, it is noticed that the definition of the critical flight mode is above the value of AoA = 14^o at Clark Y (see table), over AoA = 13^o at 14% Fauvel (Table 2), over AoA = 15^o to GOE 746 and over AoA = 9^o at Phoenix.

Table 3. Airfoils numeric values

GOE 746	*Phoenix*
[illegible]	[illegible]

As an innovative solution, a morphing profile with variable curvature values can be used to increase of the flight incidence, which leads to the delay of occurrence of the boundary layer detachment, FIG. 8, [11].

FIG. 8 Morphing airfoil

4. 3D AERODYNAMCS ANALYSIS

The flight mode of fixed lifting surfaces can be analyzed from the angle of incidence but also from slip and roll angles. These analyzes provide some aspects of the aerodynamic behavior of a classical aerodynamic aircraft (Table 4) with aerodynamic surfaces having the four aerodynamic profiles previously studied (FIG. 9) under the same flight regime (Table 5).

FIG. 9 The analyzed aircraft/glider

Table 4. Geometric parameters

Parameter	Value	Parameter	Value
Span / Lenght / High (mm)	2000 / 800 / 160	Area	0,3 m^2
Chord (mm)	150	AR	13,33

Table 5. Analysis conditions

Parameter	Value	Parameter	Value
Speed	10 m/s	Air density (ρ)	1,225 kg/m^3
AoA	-5^o÷15^o	Cinematic viscosity	1,5x10^5 m^2/s
Slip angle	0^o	Iterations	300
Roll angle	0^o	Analysis type	Fixed speed
Computational accuracy	0,01	Boundary conditions	Neumann

The concept of analysis is based on the mix of 3D panels / VLM at constant speed (10 m / s) without the inertial considerations and characteristic angles of calculation noted in Table 5. The most important coefficients for flight characteristics are shown in the following figures.

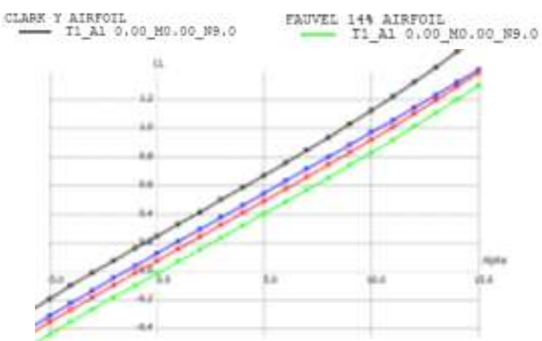

FIG. 10 C_L vs AoA

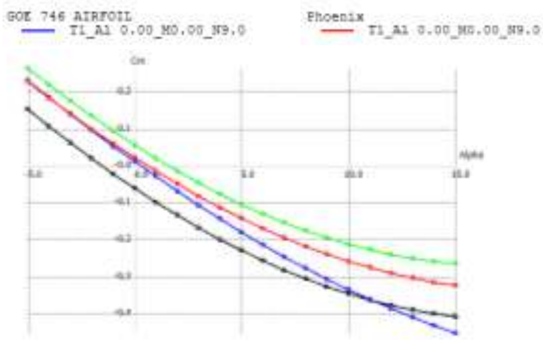

FIG. 11 C_m vs AoA

The variation of the lift coefficient C_L shown in Figure 10, shows superior performance for the Clark Y profile wing for the entire incidence range of $0^o \div 10^o$ (e.g. at AoA = 5^o we have: C_{LClark} Y = 0,66, $C_{LFauvel}$ = 0,39, $C_{LGoe746}$ = 0.54, $C_{LPhoenix}$ = 0.48). When looking at the C_m pitch coefficient (see figure 11) at the null incidence, obviously the plane with the wing having the Clark Y profile is the most unstable (eg at AoA = 0^o we have: $C_{mClarkY}$ = -0.06, $C_{mFauvel}$ = 0.055, $C_{mGoe746}$ = 0.01, $C_{mPhoenix}$ = 0.02).

The roll coefficients (FIG. 12) and slip coefficient (FIG. 13) indicate a reduced dependence on the lateral stability of the geometric configurations influenced by the use of the four analyzed profiles, the net differences increase with the increase in the incidence of flight.

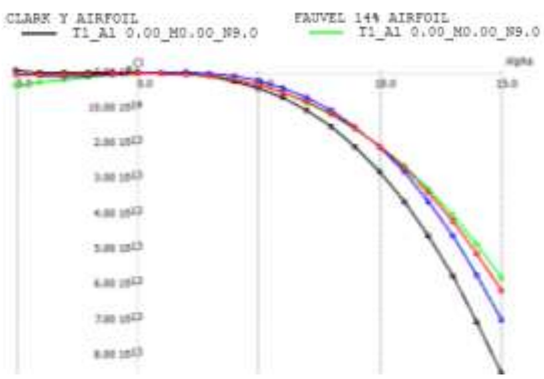

FIG. 12 C_l vs AoA

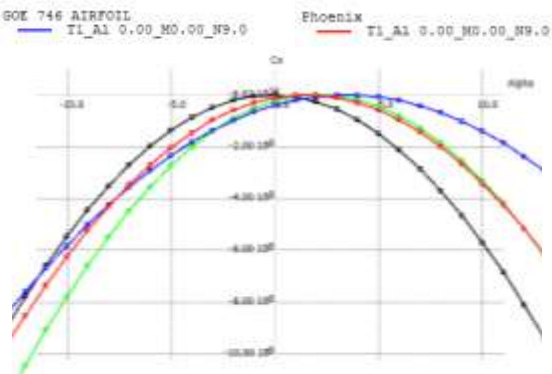

FIG. 13 C_n vs AoA

For the 3D view of the C_p pressure coefficient distribution and the drag, we use the display options for each incident angle value in the calculation range (0^o-15^o), see FIG.14 for null incidence.

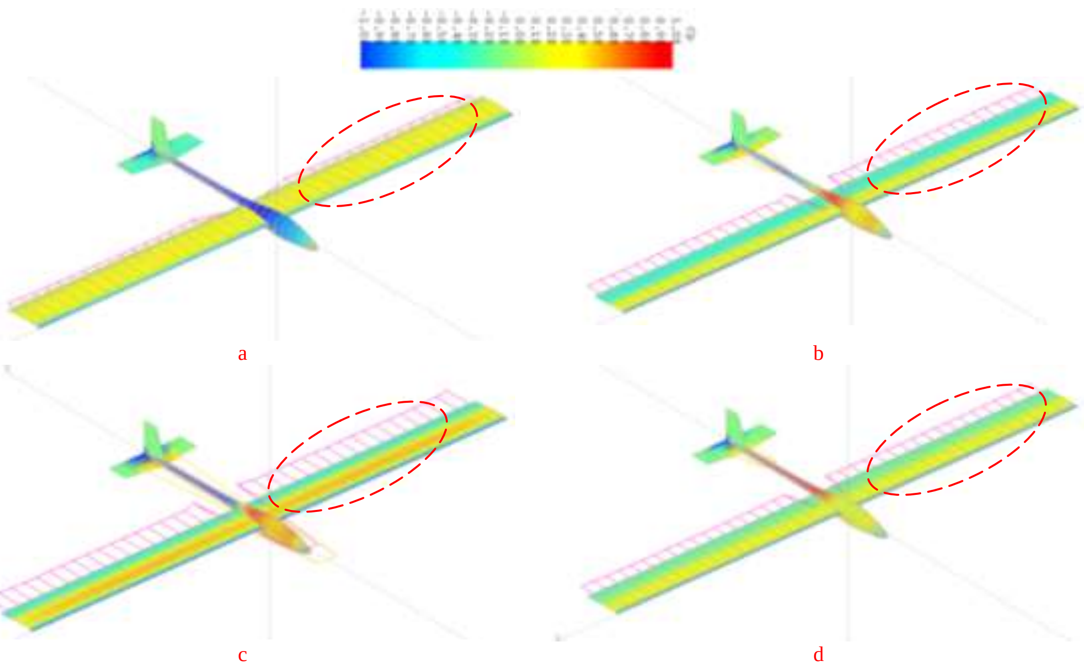

FIG. 14 The distribution of the pressure coefficient and the drag at AoA = 0^o,
a. wing with Clark Y, b. wing with Fauvel, c. wing with Goe 746, d. wing with Phoenix

FIG. 14 shows the influence of the airfoil used on the C_p distribution and the drag (eg at AoA = 0^o we have: $C_{DClark\ Y}$ = 0.004, $C_{DFauvel}$ = 0.017, $C_{DGoe746}$ = 0.022, $C_{DPhoenix}$ = 0.015).

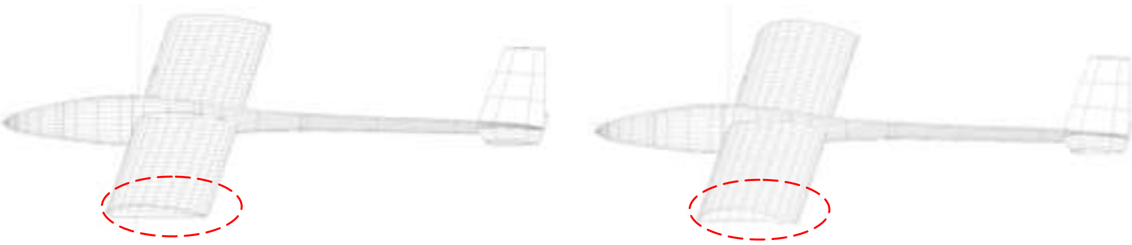

FIG. 15 Morphing wing with morphing airfoil

Starting from the 2D profile approach, the morphing concept can be used to construct 3D lifting surfaces, especially for maneuvering by adaptive control [10, 11, 12], both using morphing profiles (FIG. 15) and 3D wing torsion (FIG. 16).

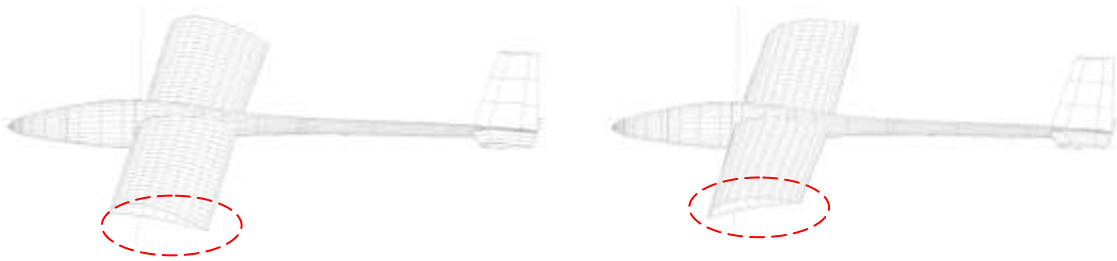

FIG. 16 Morphing wing with 3D twist

CONCLUSIONS

The article highlighted the usefulness of freeware tools in terms of both educational and exploratory exploration research for geometries that can be subjected to subsequent CFD investigations with commercial software tools. XFLR5 can be useful in the educational area to support numerically, visually and phenomenological aerodynamic concepts that are extremely useful to learners and those studying in this field.

Aerodynamic analyzes performed using software tools based on free codes can generate results that are influenced by geometric fidelity, the use of external environmental analysis conditions (air density, viscosity), geometric conditions and limitations (geometric resolution / definition points) or dynamic analysis conditions (flight velocity, incidence).

ACKNOWLEDGMENT

This article was produced with the support of the documentation of the complex project, acronym MultiMonD2, code PNIII-P1-1.2-PCDDI-2017-0637, contract 33PCCDI / 2018 funded by UEFISCDI.

REFERENCES

[1] Drela M., Yungren H., Guidelines for XFLR5 v6.03 (Analysis of foils and wings operating at low Reynolds numbers), 2011, available at http://sourceforge.net/projects/xflr5/files, accessed at 10.10.2018;

[2] Prisacariu, V., Cîrciu, I., Boşcoianu M., Flying wing aerodynamic analysis, REVIEW OF THE AIR FORCE ACADEMY, 2/2012, Braşov, Romania, ISSN 1842-9238; e-ISSN 2069-4733, p 31-35;

[3] Airfoil tools, available at http://airfoiltools.com/airfoil/details?airfoil=clarky-il, accessed at 12.10.2018;

[4] Willner M., A Tutorial of XFLR version 1, available at http://www.v0id.at/downloads/XFLR5-tut-v1.pdf accessed at 14.10.2018;
[5] Hassanalian, M., Khaki, H., & Khosravi, M. (2015). A new method for design of fixed wing micro air vehicle. Proceedings of the Institution of Mechanical Engineers, Part G: Journal of Aerospace Engineering, 229(5), 837–850. https://doi.org/10.1177/0954410014540621;
[6] Meschia, F., 2008. Model analysis with XFLR5. Radio Controlled Soaring Digest, 25(2), pp.27-51;
[7] Salam, Md Abdus. "Design, Analysis & Optimization of a Small Unmanned Aircraft.", 2015 IEEE Aerospace Conference, Big Sky, MT, USA, ISSN: 1095-323X, DOI: 10.1109/AERO.2015.7119231;
[8] M. Satyanarayana Gupta, M. Venkateswar Reddy, D. Ramana Reddy, Design and analysis of autonomous 400mm span fixed wing micro aerial vehicle, Proceedings Conference on Mechanical and Production Engineering, January 2017, in Bangkok, Thailand. ISBN: 9788193137390;
[9] http://wiki.flightgear.org/XFLR5, accessed at 15.10.2018;
[10] Mircea Boscoianu, Radu Pahonie, Adrian Coman, Some Aspects Regarding the Adaptive Control of a Flying Wing- Micro Air Vehicle with Flexible Wing Tips, WSEAS Transactions on Systems, Issue 6, Volume 7, June 2008;
[11] Prisacariu V., Boscoianu M., Cîrciu I., Morphing wing concept for small UAV, APPLIED MECHANICS AND MATERIALS, Vol. 332 (2013) pp 44-49, ISSN: 1662-7482, © (2013) Trans Tech Publications, Switzerland, doi:10.4028/www.scientific.net /AMM.332.44 OPTIROB 2013;
[12] Valasek J., Morphing aerospace vehicles and structures, Wiley 2012, ISBN 978-0-470-97286-1, 306p.